Electrochemistry Communications 98 (2019) 101–105

Contents lists available at ScienceDirect

Electrochemistry Communications

journal homepage: www.elsevier.com/locate/elecom

Full communication

Ultimate downsizing of D-fructose dehydrogenase for improving the performance of direct electron transfer-type bioelectrocatalysis

Yuya Kaida, Yuya Hibino, Yuki Kitazumi, Osamu Shirai, Kenji Kano*

Division of Applied Life Sciences, Graduate School of Agriculture, Kyoto University, Sakyo, Kyoto 606-8502, Japan

ARTICLE INFO

Keywords:
Fructose dehydrogenase
Direct electron transfer
Protein engineering
Downsizing
Redox potential shift

ABSTRACT

D-Fructose dehydrogenase (FDH), a membrane-bound heterotrimeric enzyme, shows strong activity in direct electron transfer (DET)-type bioelectrocatalysis. An FDH variant (Δ1*c*2*c*FDH) which lacks 199 amino acid residues including two heme *c* moieties from N-terminus was constructed, and its DET-type bioelectrocatalytic performance was evaluated with cyclic voltammetry at Au planar electrodes. A DET-type catalytic current of D-fructose oxidation was clearly observed on Δ1*c*2*c*FDH-adsorbed Au electrodes. Detailed analysis of the steady-state catalytic current indicated that Δ1*c*2*c*FDH transports the electrons to the electrode via heme 3*c* at a more negative potential and at more improved kinetics than the recombinant (native) FDH.

1. Introduction

Bioelectrocatalysis, which couples the electrode reaction and the catalytic function of the redox enzyme, attracts attention from the view point of environment, energy, and health [1–10]. Especially, direct electron transfer (DET)-type bioelectrocatalysis that directly couples the two reactions plays an important role in constructing mediator-free biofuel cells and biosensors with simplicity and minimum thermodynamic energy loss.

D-Fructose dehydrogenase (FDH) from *Gluconobacter japonicus* NBRC3260 is a heterotrimeric membrane protein consisting of subunit I (67 kDa), II (50 kDa), and III (20 kDa). Subunit I contains a flavin adenine dinucleotide (FAD) as the catalytic center, while subunit II contains three heme *c* moieties that we call heme 1*c*, 2*c*, and 3*c* from N-terminus of subunit II [11,12]. FDH catalyzes the oxidization of D-fructose and shows high DET-type bioelectrocatalytic activity [13]. In previous researches in our group, it was pointed out that the electron was transferred from the substrate-reduced FAD, to heme 3*c*, heme 2*c*, and an electrode, and that heme 1*c* was not involved in the catalytic electron transfer [14]. In addition, an FDH variant in which the region containing the heme 1*c* binding site was largely deleted (Δ1*c*FDH) showed an increase in the catalytic current density [15]. This was presumably due to the downsizing of the enzyme, which resulted in an increase of the surface concentration of Δ1*c*FDH.

In this study, we constructed an FDH variant which lacks 199 amino acid residues including heme 1*c* and 2*c* moieties (Δ1*c*2*c*FDH, Fig. 1) with the expectations of (1) an increase in the surface concentrations due to the downsizing and (2) the electron transfer from heme 3*c* directly to electrodes. The two expectations may lead to an increase in the limiting current density and the reduction of the over potential for the catalytic oxidation of D-fructose, respectively.

2. Experimental

2.1. Materials

Herculase II fusion DNA polymerase, restriction endonucleases and DNA ligase were purchased from Agilent Technologies (Santa Clara, CA), Takara Shuzo (Japan) and Toyobo (Japan), respectively. Other chemicals were obtained from Wako Pure Chemical Industries (Japan).

2.2. Preparation of the mutants and FDH

In the preparation of the Δ1*c*2*c*FDH mutant, in-frame deletion was introduced into plasmid pYUF3 [15]. pYUF3 is a vector pT7Blue (Novagen, Merck, USA) into which a 3.5 kbp DNA fragment corresponding to most of subunit I and all of subunit II and III are inserted. Except for the sequence containing heme 1*c* and heme 2*c*, pYUF3 was amplified by inverse polymerase chain reaction using herculase II fusion DNA polymerase. The primers used were fdhC_NSTLTKTTD(+) (5′-AATAG TACTCTGACAAAAACAACCGAT-3′) and fdhC_SignalTerminal(−) (5′-TTGCGCCCGTACGTTCGTCCCTGCGAG-3′), and the PCR product was self-ligated by Ligation-High to form pYKF1. Subsequently, PCR was carried out using pYKF1 as a template and primers UF (5′-

* Corresponding author.
E-mail address: kano.kenji.5z@kyoto-u.ac.jp (K. Kano).

https://doi.org/10.1016/j.elecom.2018.12.001
Received 28 October 2018; Received in revised form 30 November 2018; Accepted 4 December 2018
Available online 05 December 2018

N-terminal

MRYFRPLSATAMTTVLLLAGTNVRAQPTEPTPASAHRPSISRGHYLAIAADCAACHT
NGRDGQFLAGGYAISSPMGNIYSTNITPSKTHGIGNYTLEQFSKALRHGIRADGAQL
YPAMPYDAYNRLTDEDVKSLYAYIMTEVKPVDAPSPKTQLPFPFSIRASLGIWKIAAR
IEGKPYVFDHTHNDDWNRGRYLVDELAHCGECHTPRNFLLAPNQSAYLAGADIGS
WRAPNITNAPQSGIGSWSDQDLFQYLKTGKTAHARAAGPMAEAIEHSLQYLPDADI
SAIVTYLRSVPAKAESGQTVANFEHAGRPSSYSVANANSRRSNSTLTKTTDGAALYEA
VCASCHQSDGKGSKDGYYPSLVGNTTTGQLNPNDLIASILYGVDRTTDNHEILMPAF
GPDSLVQPLTDEQIATIADYVLSHFGNAQATVSADAVKQVRAGGKQVPLAKLASPGV
MLLLGTGGILGAILVVAGLWWLISRRKKRSA

C-terminal

Fig. 1. The amino acid sequence of FDH subunit II. The underlined regions were deleted. Three marked sequences (CXXCH) are the heme *c*-binding sites.

cggcctcttcgcctattacg-3′) and UR (5′- aggcaccccaggctttacac-3′), and the amplified fragment obtained was treated with *Hin*dIII and *Bam*HI to get a DNA fragment of 2.7 kbp. This DNA fragment was inserted into plasmid pSHO13 treated with *Hin*dIII and *Bam*HI to obtain pYKF2 [12]. Confirmation of nucleotide sequence of Δ1*c*2*c*FDH was entrusted to Fasmac sequencing service (Japan).

Transformation of YKF2 into *G. oxydans* NBRC12528 Δ*adhA*::Km^r was carried out by a triparental mating method, in which the HB101 strain carrying pRK2013 was used as a helper strain [16]. According to the literature [12], *Gluconobacter* cells were cultivated, with little modifications. Elution of the Δ1*c*2*c*FDH mutant from DEAE-Sepharose was performed by concentration gradient of McIlvaine buffer (McB) from 20-fold McB to 4-fold diluted McB containing 1 mM 2-mercaptoethanol and 0.1% (w/v) Triton X-100. Recombinant (native) FDH and Δ1*c*FDH were also expressed and purified in the same manner [12,15].

Sodium dodecyl sulfate-polyacrylamide gel electrophoresis (SDS-PAGE) was performed using 12.5% acrylamide gel at 100 V at room temperature, and then proteins and heme *c* were stained by Coomassie Brilliant Blue and 3,3′,5,5′-tetramethylbenzidine, respectively.

2.3. Electrochemical measurements

Cyclic voltammetry was performed with an ALS1000 electrochemical analyzer at a scan rate (v) of 10 mV s^{-1} (unless otherwise stated) and at 25 °C under anaerobic conditions in McB (pH 4.5). The working electrode was an Au planar disk electrode (3-mm diameter), which was polished to a mirror-like finish with Al_2O_3 powder (0.05-μm particle size), rinsed with distilled water, and sonicated in distilled water. The reference and counter electrodes were handmade Ag|AgCl|sat. KCl and Pt wire, respectively. A 3 μL aliquot of each enzyme solution was added to the buffer solution for measurements of bioelectrocatalytic currents. In this paper, all the potentials are referred to the reference electrode.

2.4. ESR spectroscopy

Electron spin resonance (ESR) spectra were recorded on JES-FA100 (JEOL, Japan), using a glass capillary cell with an inner diameter of 0.5 mm. The microwave power was set to 2 mW. The Δ1*c*2*c*FDH solution was concentrated to 20 μM for the measurements.

2.5. Other analytical methods

Enzyme activity was measured spectrophotometrically using potassium ferricyanide (as an electron acceptor) and the ferric dupanol reagent, as described in the literature [11].

3. Results and discussion

We constructed and purified Δ1*c*2*c*FDH. The SDS-PAGE results showed that Δ1*c*2*c*FDH was satisfactorily purified, and subunit II was reduced in size from 51 kDa to 20 kDa (data not shown), which is consistent with that predicted by the protein engineering. The heme-based enzyme concentrations were determined by spectrophotometric measurements using the molar extinction coefficient of the reduced heme *c* at 550 nm ($\varepsilon_{550\ nm}$ = 23000 M^{-1} cm^{-1} [17]), considering that the recombinant (native) FDH, Δ1*c*FDH, and Δ1*c*2*c*FDH have three, two, and one heme *c* moiety (moieties), respectively. The activities of the recombinant (native) FDH, Δ1*c*FDH, and Δ1*c*2*c*FDH were evaluated to be 2.0 × 10^{10} U mol^{-1}, 1.2 × 10^{10} U mol^{-1}, and 3.0 × 10^{9} U mol^{-1}, respectively.

Fig. 2(A) shows cyclic voltammograms (CVs) measured in the presence of D-fructose with the Au electrodes on which the recombinant (native) FDH, Δ1*c*FDH, and Δ1*c*2*c*FDH were adsorbed. A clear DET-type catalytic wave attributed to the D-fructose oxidation was observed at all of the enzyme-adsorbed electrodes. These waves were independent of the scan rate (from 1 to 50 mV s^{-1}) and the rotating speed (from 0 to 4000 rpm), indicating that the catalytic currents were independent of the mass transfer of the substrate due to a high concentration of the substrate and were controlled by the interfacial electron transfer kinetics and the enzyme kinetics [18–22].

The CVs were normalized against the current density at 0.5 V ($j_{0.5\ V}$), as shown in Fig. 2(B). The half-wave potential of the steady-state catalytic wave at the Δ1*c*2*c*FDH-adsorbed electrode was approximately 0.19 V and 0.16 V more negative than that of the recombinant (native) FDH-adsorbed electrode and Δ1*c*FDH-adsorbed electrode, respectively. Despite the downsizing of the enzyme, the $j_{0.5\ V}$ value at the Δ1*c*2*c*FDH-adsorbed electrode was slightly smaller than that at the recombinant (native) FDH-adsorbed electrode. This may be ascribed to a decrease in the surface concentration of Δ1*c*2*c*FDH probably due to a decrease in the hydrophobic property by the downsizing of the hydrophobic subunit II. Triton X-100 may in part competitively block the adsorption of Δ1*c*2*c*FDH.

Next, ESR measurements were done for Δ1*c*2*c*FDH that was reduced by D-fructose. The two-electron reduced variant yielded a strong isotropic ESR signal of an organic radical at $g \approx 2$ (data not shown). This signal is assigned to the FAD semiquinone radical. The data clearly indicate that one of the two electrons in the fully reduced FAD remains on the FAD to generate the semiquinone radical and that the other electron is transferred to heme 3*c* from the fully reduced FAD.

In addition, in order to clarify the electron transfer pathway in the DET reaction by Δ1*c*2*c*FDH, potassium cyanide (KCN) was added to the reaction buffer at a final concentration of 1 mM. The catalytic current density greatly decreased in the presence of KCN, (Fig. 2(C)). This should be due to the coordination of cyanide ion to the axial ligand of

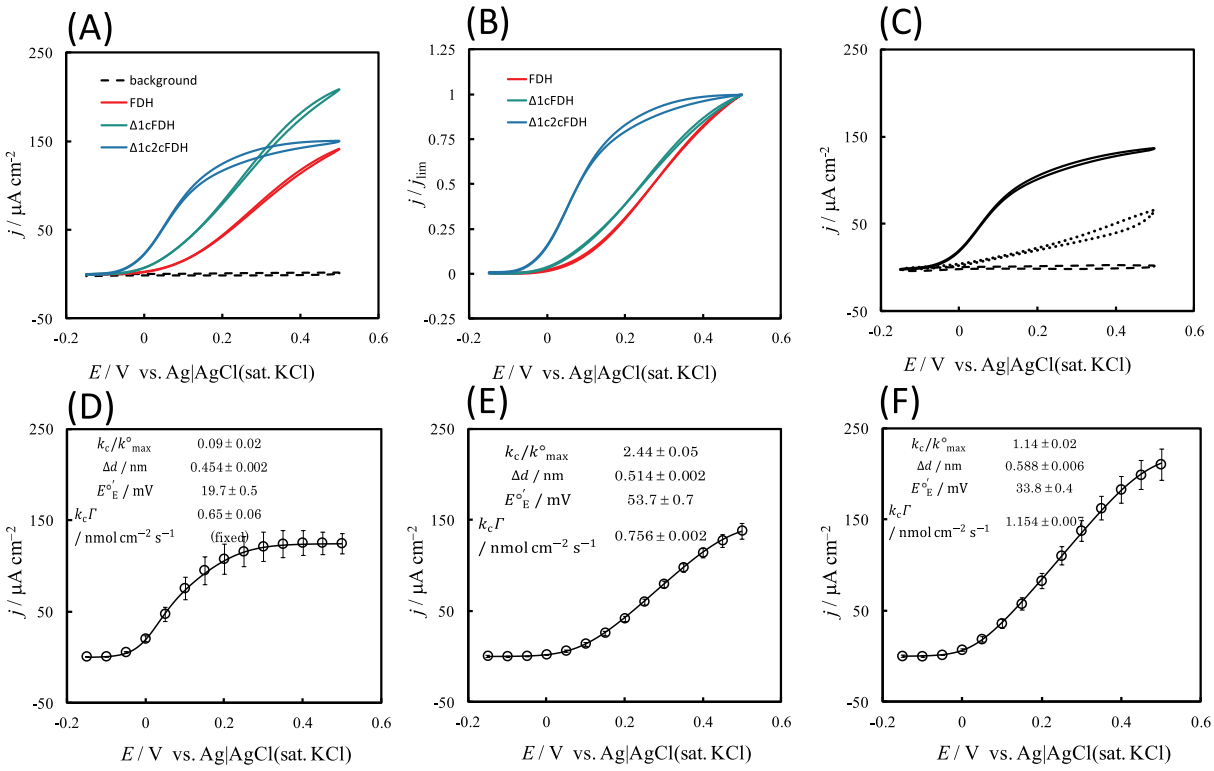

Fig. 2. (A) Original CVs and (B) normalized CVs of D-fructose oxidation at the recombinant (native) FDH-, Δ1*c*FDH-, and Δ1*c*2*c*FDH-adsorbed electrodes in McB (pH 4.5) in the presence of 100 mM D-fructose under anaerobic conditions at $\nu = 10\ \mathrm{mV\ s^{-1}}$. The broken line in panel (A) indicates the background current at the bare Au electrode. In panel (B), the background current was subtracted. In panel (C), the solid line is the CV at the Δ1*c*2*c*FDH-adsorbed electrode in McB (pH 4.5) in the presence of 100 mM D-fructose under anaerobic conditions; the broken line is background, and the dotted line is a CV after the addition of KCN (1 mM in final concentration) at $\nu = 10\ \mathrm{mV\ s^{-1}}$. Panels (D) to (F) show fitted curves obtained by non-linear least square method. The circles are the waves of the forward scan measured with (D) the Δ1*c*2*c*FDH-, (E) recombinant (native) FDH-, and (F) Δ1*c*FDH-adsorbed electrodes. The insets indicate the evaluated parameters. The Δ*d* values were obtained by assuming $\beta = 14\ \mathrm{nm^{-1}}$ [25]. The error bars were evaluated by the Student *t*-distribution at a 90% confidence level.

the heme iron, which may cause a redox potential shift of approximately 0.4 V to the negative potential direction [23]. Therefore, the electron transfer from the reduced flavin to the CN^--coordinated heme 3*c* becomes thermodynamically difficult. The very small catalytic wave was observed even in the presence of KCN. The wave showed a residual slope without sigmoidal characteristics, indicating a slow electron transfer kinetics from the CN^--treated Δ1*c*2*c*FDH to the electrode [21,22]. The possibility could not be ruled out that the electron might be transferred directly from the reduced FAD to the electrode.

Now, the steady-state catalytic waves were analyzed by considering the random orientation of the enzymes. A steady state model without the concentration polarization of the substrate was used. The following equation is given to this model [19,21]:

$$\frac{j}{j_{\mathrm{lim}}} = \frac{1}{\beta\Delta d\left(1+\exp\left\{\frac{n_{\mathrm{E}}F}{RT}(E-E^{\circ\prime}_{\mathrm{E}})\right\}\right)} \times \ln\left|\frac{k^{\circ}_{\mathrm{max}}\left(1+\exp\left\{\frac{n_{\mathrm{E}}F}{RT}(E-E^{\circ\prime}_{\mathrm{E}})\right\}\right)+k_{\mathrm{c}}\exp\left\{\frac{\alpha n_{\mathrm{E}}F}{RT}(E-E^{\circ\prime}_{\mathrm{E}})\right\}}{k^{\circ}_{\mathrm{max}}\exp(-\beta\Delta d)\left(1+\exp\left\{\frac{n_{\mathrm{E}}F}{RT}(E-E^{\circ\prime}_{\mathrm{E}})\right\}\right)+k_{\mathrm{c}}\exp\left\{\frac{\alpha n_{\mathrm{E}}F}{RT}(E-E^{\circ\prime}_{\mathrm{E}})\right\}}\right| \quad (1)$$

where n_{E} is the number of electrons in the rate determining step of the interfacial electron transfer process (=1 in this case since the number of the electron for the heme 3*c* in Δ1*c*2*c*FDH); *F*, Faraday constant; *R*, the gas constant; *T*, the absolute temperature; k°_{max}, the standard rate constant at the closest approach in the best orientation of the enzyme; Δ*d*, the distance between the closest and farthest approach of the enzyme; *α*, the transfer coefficient; *β*, the coefficient in the long range electron transfer; $E^{\circ\prime}_{\mathrm{E}}$, the formal potential of the redox center of the enzyme for electrochemical communication with electrode. The limited current density (j_{lim}) value completely controlled by the enzyme kinetics is expressed by the following equation [18–22]:

$$j_{\mathrm{lim}} = n_{\mathrm{S}}Fk_{\mathrm{c}}\Gamma \quad (2)$$

where n_{S} is the number of electrons of the substrate (=2 in this case); k_{c}, the catalytic constant; Γ, the surface concentration of the effective enzyme immobilized on the electrode.

Eqs. (1) and (2) were fitted to the wave of the forward scan at the Δ1*c*2*c*FDH-adsorbed electrode using nonlinear regression analysis by a free soft GNUPLOT with $k_{\mathrm{c}}/k^{\circ}_{\mathrm{max}}$, $\beta\Delta d$, and $E^{\circ\prime}_{\mathrm{E}}$ as adjustable parameters by setting $j_{\mathrm{lim}} = j_{0.5\ \mathrm{V}}$ and α = 0.5 (Fig. 2(D)). The waves of the forward scan at the recombinant (native) FDH- and Δ1*c*FDH-adsorbed electrodes were also analyzed in the same manner (Fig. 2(E, F)), but $k_{\mathrm{c}}\Gamma$ was also used as an adjustable parameter, because clear limiting current could not be obtained at 0.5 V. At more positive potentials than 0.5 V the catalytic currents decreased due to the formation of Au oxide layer [15].

The evaluated values of the fitting parameters of each enzyme-adsorbed electrode were given in Fig. 2((D)–(F), inset). The $k_{\mathrm{c}}/k^{\circ}_{\mathrm{max}}$ value at the Δ1*c*2*c*FDH-adsorbed electrode was much smaller than those at the other electrodes. This is probably because the distance between the active site in the variant and the electrode decreased and k°_{max} increased. The $E^{\circ\prime}_{\mathrm{E}}$ evaluated for Δ1*c*2*c*FDH (20 ± 1 mV) was more negative than those of the recombinant (native) FDH (54 ± 1 mV) and Δ1*c*FDH (34 ± 1 mV). The data support the electron transfer to the Au electrode from heme 3*c* for Δ1*c*2*c*FDH, while from heme 2*c* for the recombinant (native) and Δ1*c*FDH, as illustrated in Fig. 3. The $E^{\circ\prime}_{\mathrm{E}}$ value for the recombinant (native) FDH was very close to that spectroelectrochemically determined for heme 2*c* of the enzyme (60 ± 8 mV at pH 5.0) [24], while those of Δ1*c*2*c*FDH and Δ1*c*FDH

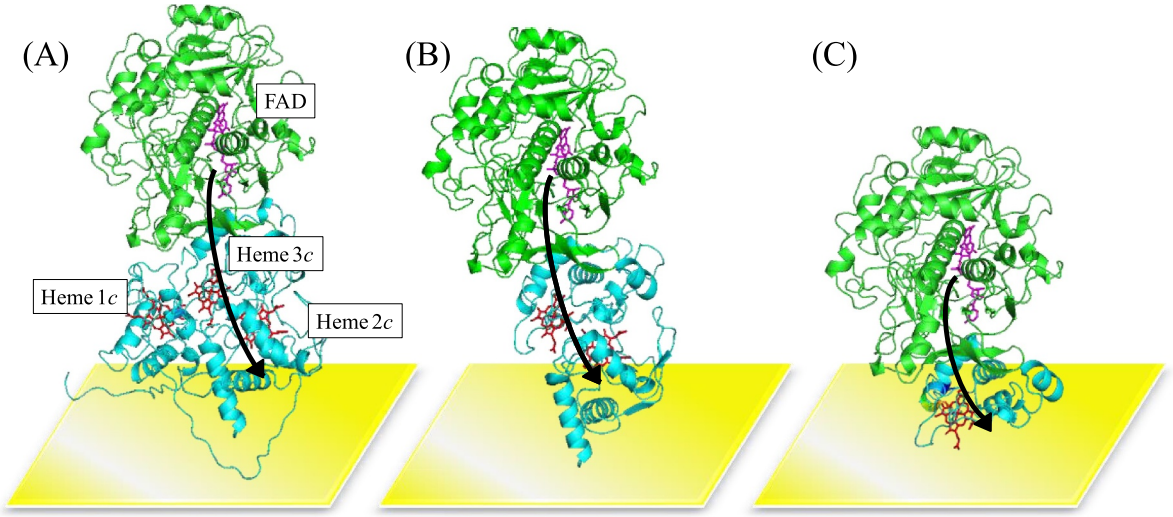

Fig. 3. Schematic of orientations suitable for DET-reaction of (A) FDH, (B) Δ1*c*FDH, and (C) Δ1*c*2*c*FDH. As templates, FAD-glucose dehydrogenase from *Aspergillus flavus* (PDB 4YNT) and thiosulfate dehydrogenase from *Marichromatium purpuratum* (PDB 5LO9) were used for subunit I (green) and II (cyan), respectively, in the homology modeling [26]. The arrow indicates the presumable pathway of the electron transfer in the DET-type reaction. The subunit III was not shown in the modeling because of lack of the structural information of similar proteins. (For interpretation of the references to colour in this figure legend, the reader is referred to the web version of this article.)

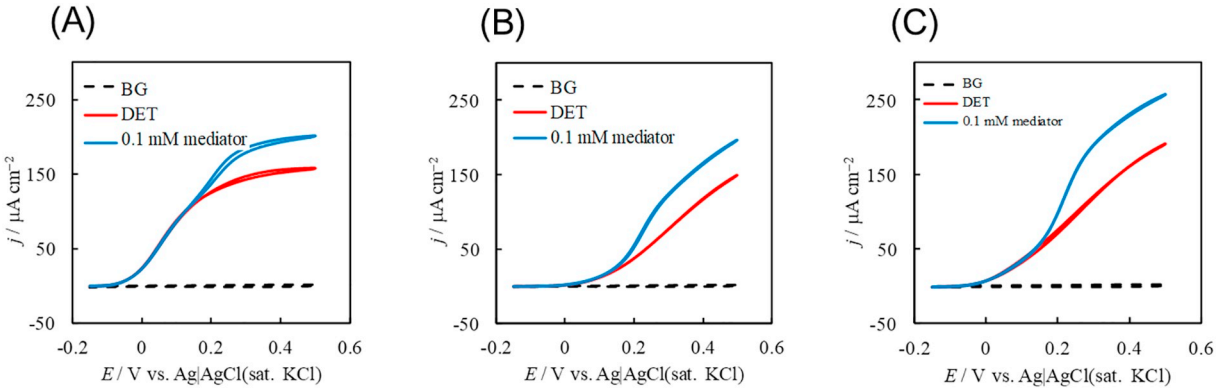

Fig. 4. Comparison of MET- and DET-type responses at (A) the Δ1*c*2*c*FDH-, (B) recombinant (native) FDH-, and (C) Δ1*c*FDH-adsorbed electrodes. The experimental conditions were identical with those given in Fig. 2 (A), except the presence of 0.1 mM $K_4[Fe(CN)_6]$.

were slightly more positive than the spectroelectrochemically determined ones of heme 3*c* (−10 ± 4 mV) and heme 2*c* for the recombinant (native) FDH. The mutation seems to cause change in the environment around the heme moiety in the variant. The relative values of $k_c\Gamma$ were 1: 1.15: 1.74 for Δ1*c*2*c*FDH-, recombinant (native) FDH, and Δ1*c*FDH. The value of Γ could not be separately evaluated, but was indirectly compared by measuring mediated electron transfer (MET)-type bioelectrocatalytic wave. MET-type-bioelectrocatalytic wave was superimposed on the DET-type wave at potentials more positive than 0.2 V on the addition of $K_4[Fe(CN)_6]$ as a mediator (Fig. 4). The relative heights of the limiting MET-type waves (the remaining limiting currents after subtraction of the DET-type currents) were 1: 1.1: 1.8 for Δ1*c*2*c*FDH-, recombinant (native) FDH, and Δ1*c*FDH. The ratio is close to that of $k_c\Gamma$. Therefore, the ratio of $k_c\Gamma$ seems to reflect the ratio of Γ at almost constant k_c. On the other hand, the mutation did not lead to a big difference in Δd, suggesting that the extent of the random orientation seems to be similar to each other. All these quantitative considerations support the proposed schematic of the productive orientation of the enzymes (Fig. 3). The increase of k°_{max} in the Δ1*c*2*c*FDH mutant seems to be attributed to a decrease in the distance between the electrochemically communicating heme and the electrode.

4. Conclusions

We successfully constructed the Δ1*c*2*c*FDH variant that lacks 199 amino acid residues including heme 1*c* and 2*c*. The Δ1*c*2*c*FDH variant showed bioelectrocatalytic wave for D-fructose oxidation at the planar gold electrode. In the DET reaction of Δ1*c*2*c*FDH, the electrons were transferred from D-fructose to the electrode via FAD and heme 3*c* in this order. The Δ1*c*2*c*FDH variant transferred the electrons to the electrode at a more negative potential than the recombinant (native) FDH (Fig. 3). Therefore, the energy loss in the DET-type bioelectrocatalysis of FDH successfully decreased. The interfacial electron transfer kinetics were also improved probably by shortening the distance between heme *c* and the electrode. However, the maximum current density decreased, which is opposite to what we expected from the downsizing mutation. This seems to be due to a decrease in the hydrophobicity of the variant.

Acknowledgements

This work was supported by Research Fellowships of Japan Society for the Promotion of Science for Young Scientists (to Y. H., #201708760).

References

[1] N. Mano, A. de Poulpiquet, O_2 reduction in enzymatic biofuel cells, Chem. Rev. 118 (2018) 2392–2468, https://doi.org/10.1021/acs.chemrev.7b00220.

[2] I. Mazurenko, A. de Poulpiquet, E. Lojou, Recent developments in high surface area bioelectrodes for enzymatic fuel cells, Curr. Opin. Electrochem. 5 (2017) 74–84, https://doi.org/10.1016/j.coelec.2017.07.001.

[3] K. Kano, T. Ikeda, Fundamentals and practices of mediated bioelectrocatalysis, Anal. Sci. 16 (2000) 1013–1021, https://doi.org/10.2116/analsci.16.1013.

[4] V. Fourmond, C. Léger, Modelling the voltammetry of adsorbed enzymes and molecular catalysts, Curr. Opin. Electrochem. 1 (2017) 110–120, https://doi.org/10.1016/j.coelec.2016.11.002.

[5] J. Wang, Electrochemical glucose biosensors, Chem. Rev. 108 (2007) 814–825, https://doi.org/10.1016/B978-012373738-0.50005-2.

[6] C. Léger, P. Bertrand, Direct electrochemistry of redox enzymes as a tool for mechanistic studies, Chem. Rev. 108 (2008) 2379–2438, https://doi.org/10.1021/cr0680742.

[7] D. Leech, P. Kavanagh, W. Schuhmann, Enzymatic fuel cells: recent progress, Electrochim. Acta 84 (2012) 223–234, https://doi.org/10.1016/j.electacta.2012.02.087.

[8] F.A. Armstrong, G.S. Wilson, Recent developments in faradaic bioelectrochemistry, Electrochim. Acta 45 (2000) 2623–2645, https://doi.org/10.1016/S0013-4686(00)00342-X.

[9] F.A. Armstrong, H.A.O. Hill, N.J. Walton, Direct electrochemistry of redox proteins, Acc. Chem. Res. 21 (1988) 407–413, https://doi.org/10.1021/ar00155a004.

[10] J.A. Cracknell, K.A. Vincent, F.A. Armstrong, Enzymes as working or inspirational electrocatalysts for fuel cells and electrolysis, Chem. Rev. 108 (2008) 2439–2461, https://doi.org/10.1021/cr0680639.

[11] M. Ameyama, E. Shinagawa, K. Matsushita, O. Adachi, D-fructose dehydrogenase of *Gluconobacter industrius*: purification, characterization, and application to enzymatic microdetermination of D-fructose, J. Bacteriol. 145 (1981) 814–823.

[12] S. Kawai, M. Goda-Tsutsumi, T. Yakushi, K. Kano, K. Matsushita, Heterologous overexpression and characterization of a flavoprotein-cytochrome c complex fructose dehydrogenase of *Gluconobacter japonicus* NBRC3260, Appl. Environ. Microbiol. 79 (2013) 1654–1660, https://doi.org/10.1128/AEM.03152-12.

[13] T. Ikeda, F. Matsushita, M. Senda, D-fructose dehydrogenase-modified carbon paste electrode containing p-benzoquinone as a mediated amperometric fructose sensor, Agric. Biol. Chem. 54 (1990) 2919–2924, https://doi.org/10.1080/00021369.1990.10870394.

[14] Y. Hibino, S. Kawai, Y. Kitazumi, O. Shirai, K. Kano, Mutation of heme *c* axial ligands in D-fructose dehydrogenase for investigation of electron transfer pathways and reduction of overpotential in direct electron transfer-type bioelectrocatalysis, Electrochem. Commun. 67 (2016) 43–46, https://doi.org/10.1016/j.elecom.2016.03.013.

[15] Y. Hibino, S. Kawai, Y. Kitazumi, O. Shirai, K. Kano, Construction of a protein-engineered variant of D-fructose dehydrogenase for direct electron transfer-type bioelectrocatalysis, Electrochem. Commun. 77 (2017) 112–115, https://doi.org/10.1016/j.elecom.2017.03.005.

[16] D.H. Figurski, D.R. Helinski, Replication of an origin-containing derivative of plasmid RK2 dependent on a plasmid function provided in trans, Proc. Natl. Acad. Sci. U. S. A. 76 (1979) 1648–1652, https://doi.org/10.1073/pnas.76.4.1648.

[17] J. Marcinkevicienc, G. Johansson, Kinetic studies of the active sites functioning in the quinohemoprotein fructose dehydrogenase, FEBS Lett. 318 (1993) 23–26, https://doi.org/10.1016/0014-5793(93)81319-U.

[18] K. So, Y. Kitazumi, O. Shirai, K. Kano, Analysis of factors governing direct electron transfer-type bioelectrocatalysis of bilirubin oxidase at modified electrodes, J. Electroanal. Chem. 783 (2016) 316–323, https://doi.org/10.1016/j.jelechem.2016.10.062.

[19] H. Xia, Y. Kitazumi, O. Shirai, K. Kano, Enhanced direct electron transfer-type bioelectrocatalysis of bilirubin oxidase on negatively charged aromatic compound-modified carbon electrode, J. Electroanal. Chem. 763 (2016) 104–109, https://doi.org/10.1016/j.jelechem.2015.12.043.

[20] Y. Sugimoto, Y. Kitazumi, O. Shirai, M. Yamamoto, K. Kano, Role of 2-mercaptoethanol in direct electron transfer-type bioelectrocatalysis of fructose dehydrogenase at Au electrodes, Electrochim. Acta 170 (2015) 242–247, https://doi.org/10.1016/j.electacta.2015.04.164 (Electrochimica acta).

[21] C. Léger, A.K. Jones, S.P.J. Albracht, F.A. Armstrong, Effect of a dispersion of interfacial electron transfer rates on steady state catalytic electron transport in [NiFe]-hydrogenase and other enzymes, J. Phys. Chem. B 106 (2002) 13058–13063, https://doi.org/10.1021/jp0265687.

[22] C. Léger, A.K. Jones, W. Roseboom, S.P.J. Albracht, F.A. Armstrong, Enzyme electrokinetics: hydrogen evolution and oxidation by *Allochromatium vinosum* [NiFe]-hydrogenase, Biochemistry 41 (2002) 15736–15746, https://doi.org/10.1021/bi026586e.

[23] I. Taniguchi, Y. Mie, K. Nishiyama, V. Brabec, O. Novakova, S. Neya, N. Funasaki, Electrochemistry of monoazahemin reconstituted myoglobin at an indium oxide electrode, J. Electroanal. Chem. 420 (1997) 5–9.

[24] S. Kawai, T. Yakushi, K. Matsushita, Y. Kitazumi, O. Shirai, K. Kano, The electron transfer pathway in direct electrochemical communication of fructose dehydrogenase with eelectrodes, Electrochem. Commun. 38 (2014) 28–31.

[25] C.C. Moser, J.M. Keske, K. Warncke, R.S. Farid, P.L. Dutton, Nature of biological electron transfer, Nature 355 (1992) 796–802.

[26] P. Bollella, Y. Hibino, K. Kano, L. Gorton, R. Antiochia, The influence of pH and divalent/monovalent cations on the internal electron transfer (IET), enzymatic activity and structure of fructose dehydrogenase, Anal. Bioanal. Chem. 410 (2018) 3253–3264.